Supplementary Information (SI) for Journal of Materials Chemistry A.

# Supporting Information

# Construction of ionic cavities in porous aromatic frameworks for palladium immobilization and effective catalysis

Yuhui Zhai[a], Zhaofu Zhang[b], Hengtao Lei[b], Tingting Ma[b], Mengnan Gu[b], Yuyang Tian*[b], XiaoYu Cao*[a]

a. School of Chemistry and Chemical Engineering, Henan University of Technology, Zhengzhou 450001, China. E-mail: caoxy@haut.edu.cn

b. Key Laboratory of Polyoxometalate and Reticular Material Chemistry of Ministry of Education, Faculty of Chemistry, Northeast Normal University, Changchun 130024, China. E-mail: tianyy100@nenu.edu.cn

## 1 Materials and Characterization

FT-IR spectra were carried out using a Nicolet IS50 Fourier transform infrared spectrometer. $^1$H NMR spectrum of 3-(4-bromobenzyl)-1-methyl-1H-imidazole was performed on a Bruker Avance III model 400 MHz NMR spectrometer at a MAS rate of 5 kHz. Scanning electron microscopy (SEM) was tested with a Hitachi SU8010 field-emission scanning electron microscope. The transmission electron microscopy (TEM) was obtained from JEOL JEM 3010. The surface area and pore size distribution were determined using an Autosorb iQ2 AbsorptoMeter, Quanta chrome Instrument. Elemental analysis was performed by an inductively coupled plasma atomic emission spectrometer (ICP-AES) Prodigy. Thermogravimetric analysis (TGA) was performed on a METTLER-TOLEDO TGA/DSC 3+ analyser with a heating rate of 10 °C min$^{-1}$ under air flow. X-ray photoelectron spectroscopy (XPS) measurements were obtained with an Escalab-MK II photoelectronic spectrometer with Al Kα (1200 eV). Gas Chromatography Mass Spectrometry (GC-MS) analysis was used to analyze the catalytic products by using a Thermo Scientific Trace 1310-ISQ 7000 system.

## 2 Synthetic procedure

### 2.1 Synthesis of the 3-(4-bromobenzyl)-1-methyl-1H-imidazole (3-BMHI):

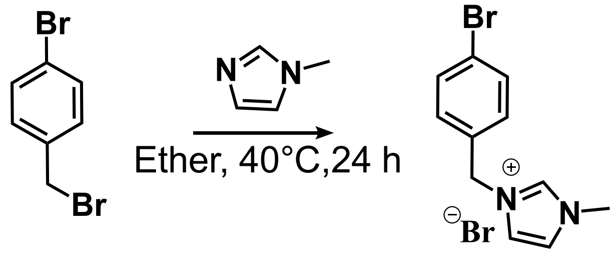

**Fig. S1** The synthesis schematic of 3-(4-bromobenzyl)-1-methyl-1H-imidazole (3-

BMHI).

Due to the different solubility of the monomers, this paper refers to the reported articles and adapts the synthesis method[1]. 4-Bromobenzyl bromide (249 mg, 1 mmol) and N-methylimidazole (98.6 mg, 1.2 mmol) were added into a 50 mL flask sequentially, and 40 mL of ether was added to fully sonicate to fully dissolve the two monomers, and then stirred at reflux at 40°C for 24 h. After the system was cooled down to room temperature, the precipitated white solids were washed with ethyl acetate, and dried under vacuum to obtain the white solid powder (321 mg, 98% yield). white solid powder was obtained after vacuum drying (321 mg, 98% yield). The $^1$H NMR hydrogen spectrum of the 3-(4-bromobenzyl)-1-methyl-1H-imidazole was shown in Fig. S2. $^1$H NMR (500 MHz, DMSO): δ 9.24 (1H, Imidazol-H), 7.81 (1H, Imidazol-H), 7.74 (1H, Imidazol-H), 7.65 (2H, Ar-H), 7.41 (2H, Ar-H)), 5.43 (2H, trityl Ar-H). 3.86 (1H, $CH_3$).

## 3 General procedure for Suzuki-Miyaura coupling reaction:

Bromobenzene (1 mmol), phenylboronic acid (1.2 mmol), PAF-282-$Pd^{2+}$ (10 mg, 0.5 mol%), Biphenyl (1 mmol), potassium carbonate (330 mg, 2.4 mmol) were added to a 25 mL Schlenk tube. Subsequently, 5 mL ethanol and 5 mL water were added and reacted at 80°C for 6 h. When the reaction system is cooled to room temperature, the reaction mixture is filtered to recover the solid catalyst. The samples were washed with methanol, ethanol and other organic solvents, vacuum dried at 60°C and used for the next cycle experiment. The organic phase after filtration was extracted with dichloromethane, dried with anhydrous sodium sulfate, and the cyclic yield of Suzuki-Miyaura was calculated by gas chromatography-mass spectrometry.

## 3. Characterizations

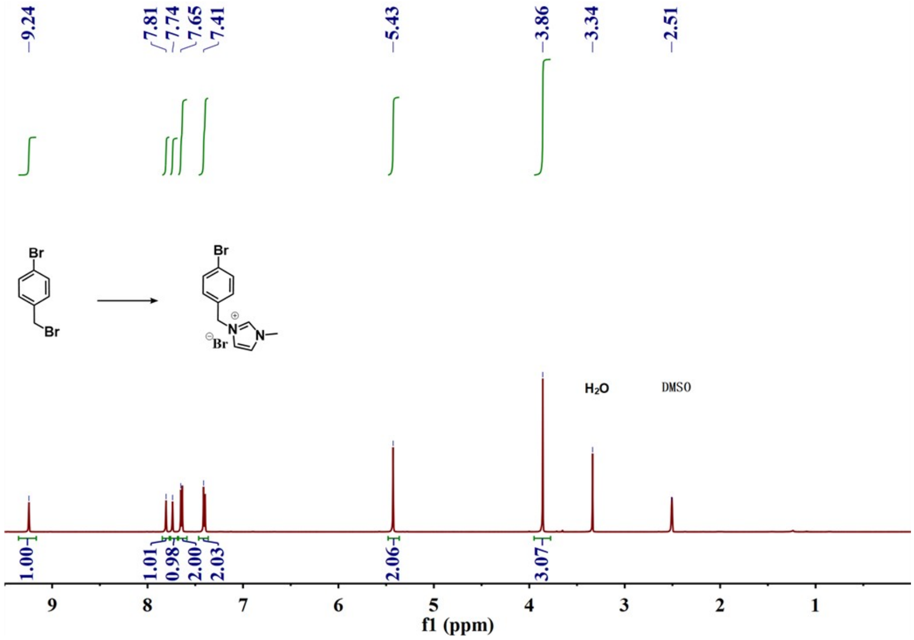

**Fig. S2** $^1$H NMR of 3-(4-bromobenzyl)-1-methyl-1H-imidazole with the solvent of DMSO.

**Fig. S3** The FT-IR spectra of PAF-282 and PAF-282-Pd$^{2+}$(a) and spectra from 2000 cm$^{-1}$ to 480 cm$^{-1}$ (b).

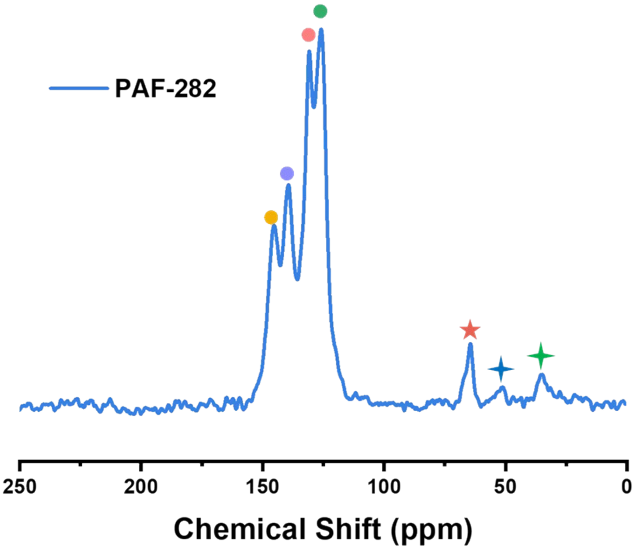

**Fig. S4** $^{13}$C NMR spectrum of PAF-282.

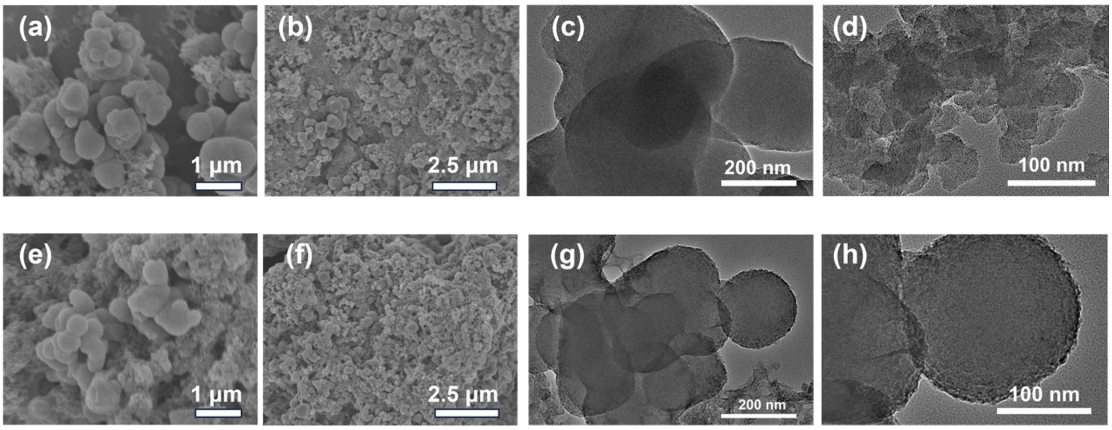

**Fig. S5** The SEM images (a-b) and TEM images (c-d) of PAF- 282. The SEM images (e-f) and TEM images (g-h) of PAF- 282-Pd$^{2+}$.

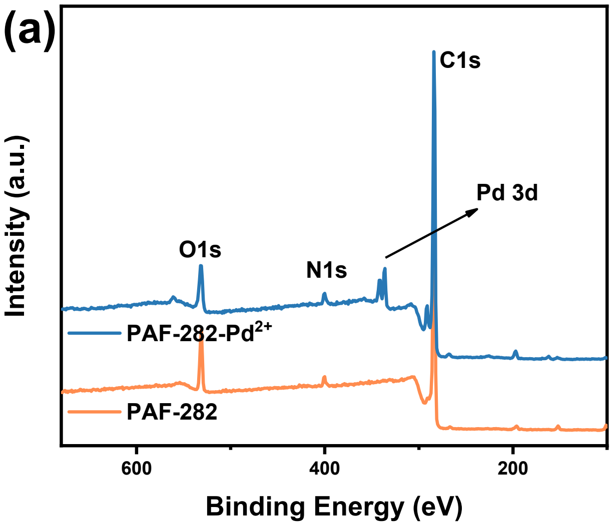

**Fig. S6** XPS spectrum of PAF-282 and PAF-282-Pd$^{2+}$.

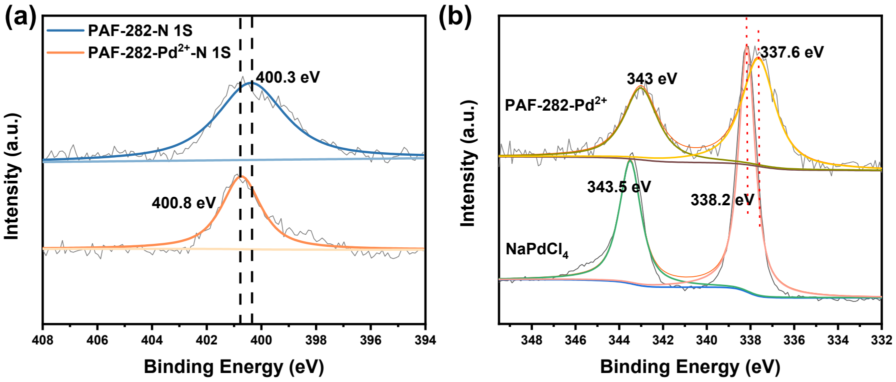

**Fig. S7** (a) N 1s spectra of PAF-282 and PAF-282-Pd$^{2+}$. (b) XPS spectrum of Pd in PAF-282-Pd$^{2+}$.

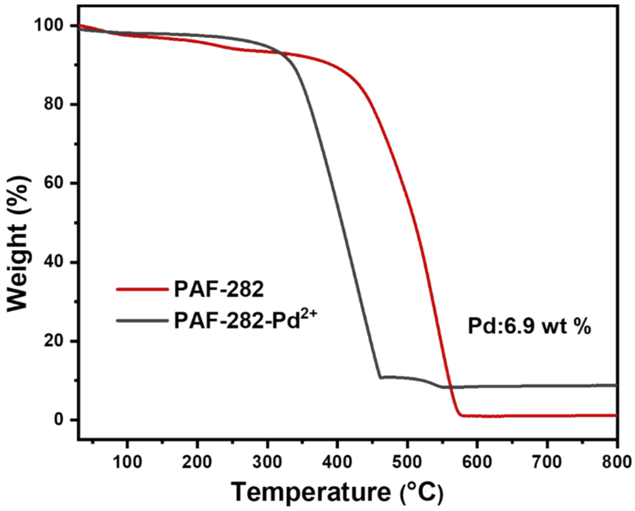

**Fig. S8** The TGA curves of PAF-282 and PAF-282-$Pd^{2+}$.

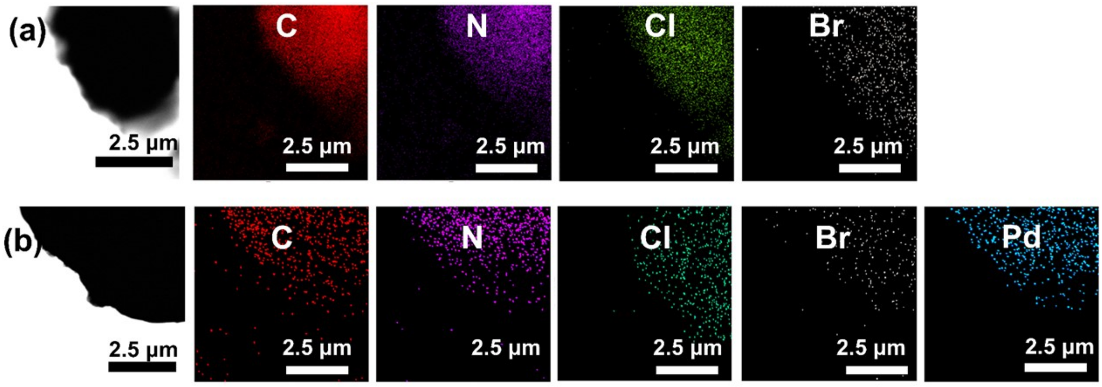

**Fig. S9** EDS mapping of PAF-282 (a) and PAF-282-$Pd^{2+}$ (b).

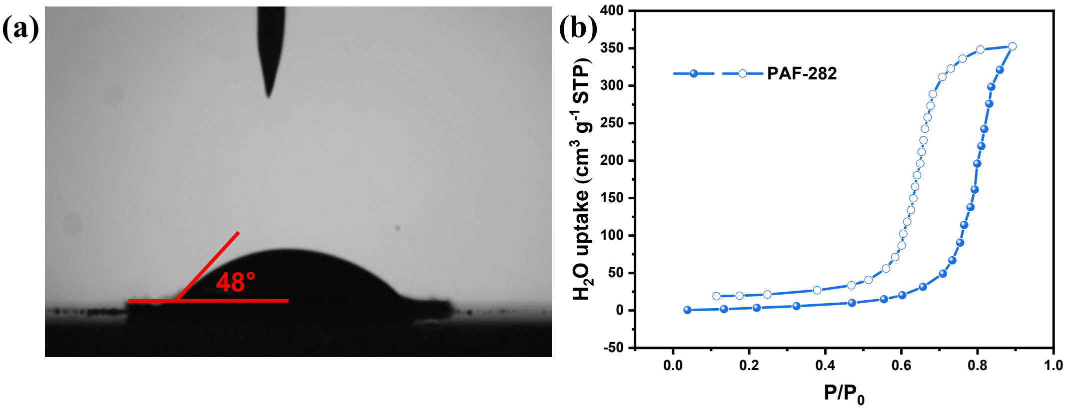

**Fig. S10** The water contact angle meter (a) and water vapor adsorption of PAF-282 (b).

**Table S1** Elemental analytical content of CNH.

| EA | C | N | H |
|---|---|---|---|
| Theoretical | 88.29 | 2.39 | 6.3 |
| Experiment | 83.29 | 2.44 | 5.8 |

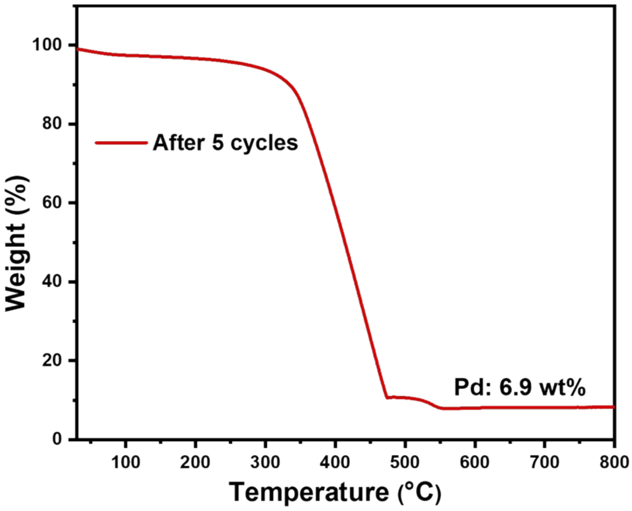

**Fig. S11** The TGA curves of PAF-282-Pd$^{2+}$ after 5 cycles.

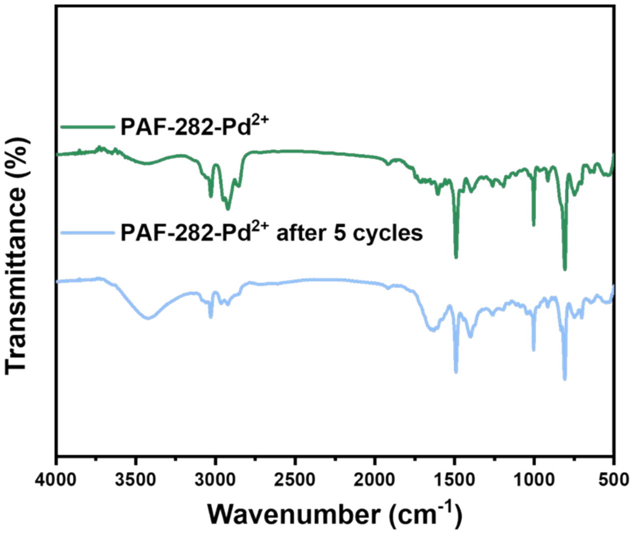

**Fig. S12** The FT-IR spectra of PAF-282-Pd$^{2+}$ after 5 cycles.

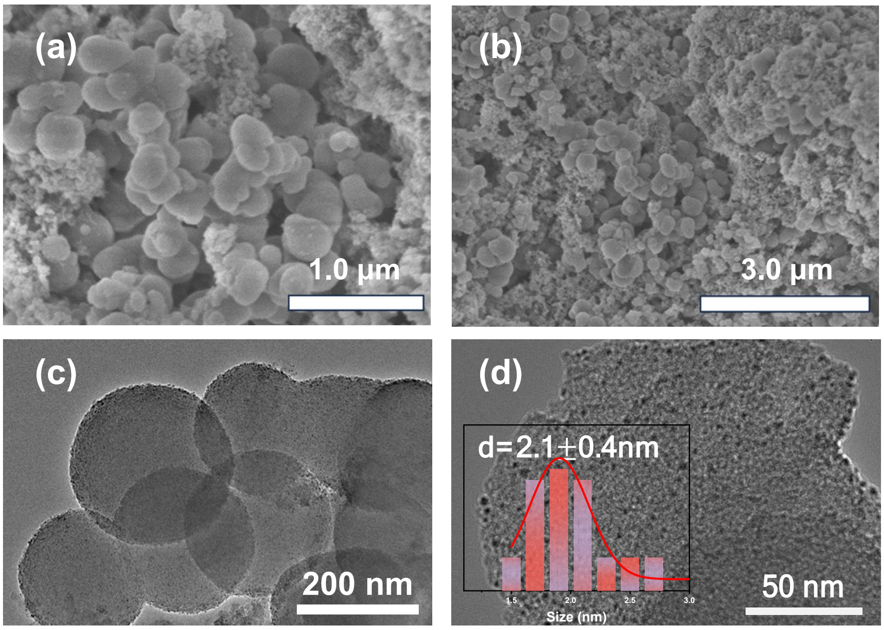

**Fig. S13** The SEM images (a-b) and TEM images (c-d) of PAF-282-Pd$^{2+}$ after 5 cycles.

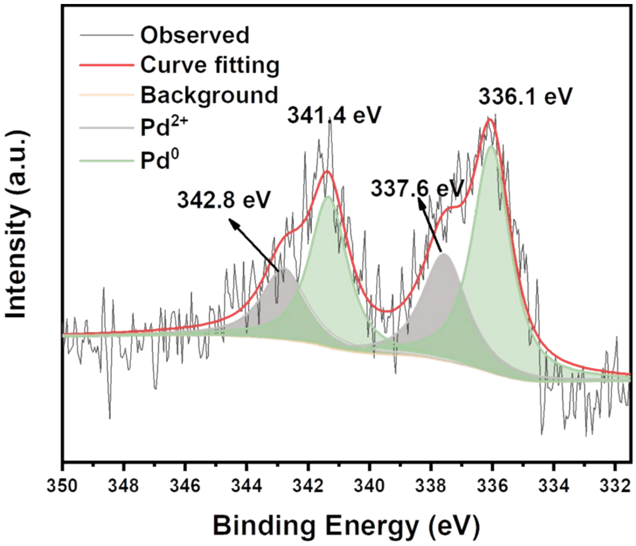

**Fig. S14** XPS spectrum of Pd in PAF-282-Pd$^{2+}$ after 5 cycles.

**Table S2** Reported TOF of porous materials catalyzed Suzuki reaction of bromobenzene.

| Cat. | TOF [$h^{-1}$] | ref |
|---|---|---|
| PAF-282-$Pd^{2+}$ | 9100 | Our work |
| Pd@CNPCs | 327 | Chem. Mater., 2011, **23**, 5243-5249 |
| Pd@COF-LZU1 | 64 | J. Am. Chem. Soc., 2011, **133**, 19816. |
| Pd-CIN-1 | 980 | Dalton Trans., 2012, **41**, 1304-1311. |
| MsMOP-1 | 319 | J. Mater. Chem. A, 2013, **1**, 14108. |
| Pd/MPP | 960 | *Small*, 2013, 9, 2460. |
| Pd(0)/M CoS-1 | 102 | *Appl. Catal., A*, 2014, **469**, 320-327 |
| PPI-1-NPy-Pd | 450 | *Green Chem.*, 2015, **17**,466-473. |
| PPI-2-NPy-Pd | 580 | *Green Chem.*, 2015, **17**,466-473. |
| Pd(II)@bbp-MOP | 1450 | *Macromol . Rapid Commun.*, 2015, **36**, 413-418. |
| Pd(OAC)2@COF-300 | 3000 | *ChemCatChem*, 2016, **8**, 743-750. |
| Pd/POP | 219 | *Chin. J. Chem.*, 2016, **34**, 373-380. |
| Bpy-Pd-POP-1 | 248 | *RSC Adv.*, 2016, **6**, 34866-34871. |
| Bpy-Pd-POP-2 | 246 | *RSC Adv.*, 2016, **6**, 34866-34871. |
| Pd@NHC-MOP | 248 | *ChemistrySelect*, 2016, **1**, 1371-1376. |
| Pd/Cy-pip | 88 | *Ind. Eng. Chem. Res.*, 2017, **56**, 4275-4280. |
| PAF-70-Pd | 28800 | Chem. Sci., 2018, **9**, 3523 |
| Pd@K-ZSM-5 | 63 | Catal. Today, 2023, **410**, 237-246. |
| 0.5Pd/HS-1 | 14 | Appl. Surf. Sci., 2024, 659, 159904. |
| Pd@USY | 6667 | Ind. Eng. Chem. Res. 2020, **59**, 11241–11249 |
| Pd@USY-$NaBH_4$ | 400 | Ind. Eng. Chem. Res. 2020, **59**, 11241–11249 |

## References

[1] Ma T, Zhao R, Song J, et al. Turning Electronic Waste to Continuous-Flow Reactor Using Porous Aromatic Frameworks[J]. ACS Appl. Mater. Interfaces, 2022, 14(22): 25601-25608.